Engineering and Technology Journal e-ISSN: 2456-3358

Volume 10 Issue 05 May-2025, Page No.- 4834-4846

DOI: 10.47191/etj/v10i05.13, I.F. – 8.482

Thermo-Kinetics of The Sun Drying of Plantain Slices Under Forced Convections and Open Air Conditions

Clement A. Komolafe[1], Edward E. Essoun[1,2], David Abaidoo[1,2], Patrick K. Amissah[1,2], Omotola J. Komolafe[3]

[1]Department of Mechanical Engineering, Faculty of Engineering, University of Mines and Technology, P.O.B. 237, Tarkwa, Ghana, West Africa.

[2]Department of Mechanical Engineering, Faculty of Engineering, Takoradi Technical University, P.O.B. 256, Takoradi, Ghana, West Africa.

[3]Department of Electrical and Electronics Engineering, Ekiti State University, P.M.B.5363, Ado Ekiti, Nigeria

ABSTRACT: The thermo kinetics of the sun drying of plantain slices integrated with the granite sensible thermal energy storage material (GSTESM) were investigated. Fifteen (15) thin layer drying models were adopted to model the drying curves following standard criteria for fitness. The moisture content of plantain slices took 1140 minutes for both open air and solar drying system with plywood drying chamber to reduce from 61.5% to 6.83 and 7.34% w.b. respectively, while it took the solar drying system with Perspex glass chamber 1080 minutes to reduce the same initial moisture content of plantain slices to 6.13%. The effective moisture diffusivities for plantain slices were 17.825 x 10^{-10}, 14.880 x 10^{-10} and 13.662 x 10^{-10} for the controlled solar dyers (with Perspex glass chamber, plywood chamber) and open air respectively. The obtained activation energy values for the three drying processes (solar drying with Perspex and plywood chambers) and open air were 22.641, 22.144 and 21.983 kJ/mol. The values of mass transfer coefficient for the dried plantain slices in the solar drying systems (with Perspex and plywood chambers) and open air were 1.246 x 10-6, 1.435 x 10^{-6}, 1.966 x 10-6 m/s respectively. While the heat transfer coefficients were 3.165, 3.0412 and 2.751 W/m2. K. Midilli et al. performed better than the others in describing the drying behavior of the solar drying system of plantain slices using the Perspex glass and plywood chamber, while the model proposed by logarithmic performed better than the others in describing the open air behaviour of plantain slices. Therefore, the obtained results would be useful in the design of solar drying equipment for agricultural products under open air and forced convection mode.

KEYWORDS: Modelling; forced convection; sun drying; thermal energy storage material; plantain slices

1.0 INTRODUCTION

The use of sustainable postharvest technologies for the keeping of fresh foodstuffs and other perishable agricultural products in a stable condition over a long period after harvesting has been identified as one of the major ways for combating food shortage worldwide. One of these perishable agricultural products is plantain (Musa paradisiaca). More than 70 million people in Africa rely on plantains for more than 25% of their daily carbohydrate needs [1]. In Nigeria and most of the other West African countries, the unripe plantain can be traditionally processed directly into food by roasting and boiling. Also, it can be processed into paste and powder (Elubo) for the production of a solid food called 'Amala' in the south-western part of Nigeria. The major operation to be carried out before plantain is processed into flour is drying. Early plantain processing researchers found that over 40% of the collected fruit is discarded, resulting in an approximate 11% economic loss. One of the most important post-harvest techniques or technologies used worldwide to increase the shelf life of agricultural products and reduce spoilage is drying. It is a thermophysical and physicochemical action whose dynamic principles are governed by heat and moisture transfer laws within and outside the grains of material being dried[2]. Eliminating moisture prevents the growth and production of microorganisms that cause deterioration and reduces many of the deteriorative responses that moisture mediates[3]. Other important objectives of drying operations are weight and volume reduction, thus decreasing transportation and storage costs [4]. Determining the drying rates is crucial for creating reliable process models since the drying kinetics are used to explain the moisture removal processes and their reliance on the process factors[5]. The drying rate of agricultural products falls under two stages, namely, the constant rate period and the falling rate period. The movement of the moisture within the material takes place because of diffusion, cell contraction and vapour pressure gradient between the material and its drying medium[2]. Drying being a basic unit operation in several industrial applications, requires a substantial amount of energy; therefore constitutes one of the main energy intensive processes[6]. It is a complex thermal process involving heat and moisture transfer. Traditionally, the open sun drying is widely used because it is cheap. However, although this method is labour intensive and time consuming, it is also susceptible to several other problems such as pest infestation, animal intrusion, and an inability to manage the drying rate etc. [7-11]. To alleviate people from the above shortcomings of the open sun drying, mechanical and solar dryers have been proposed as viable alternatives to sun drying because of their better dried products and quicker drying durations[3, 12]. The major stakeholders in the farm business who are small scale farmers, live in rural areas and cannot afford the use of mechanical drying technologies because of their high initial investment cost and operation expenses. These methods are primarily utilized in industrialized countries. The use of solar energy is more preferable to mechanical technologies because it is less expensive, renewable in nature, and readily available. In addition, its commercial feasibility and positive environmental consequences make it a desirable option for farmers in rural areas [13]. However, problems with intermittency, moisture resorption, and weather dependence have been linked to the solar drying process [14]. As a way out of these problems, integration of thermal energy storage materials, which have been classified into sensible, latent heat and thermochemical or their combination, has been identified[15]. Among these heat storage materials, sensible heat storage materials include sand, rock, pebbles, bricks, refractories, and gravel[3, 6, 16]. Considering their abundance in the rural areas where the main stakeholders (farmers) reside, these resources are more easily accessible, affordable, and readily available than the other two types. It has been noted that due to its affordability, farmers in rural regions continue to favour the conventional open sun drying approach over other drying methods. However, a practical substitute for open sun drying will be the integration of sensible heat storage materials into the low-cost and straightforward solar drying systems[3].

Studies on the drying kinetics of plantain using different methods have been documented [17-23]. Research on the integration of thermal energy storage materials into the solar/sun drying process of plantain slices using three different experimental setups concurrently is seems unavailable. Also, information regarding the comparative data for the drying parameters during sun/solar drying of plantain slices using three experimental setups (open sun and two solar drying systems).

Thus, the observed research gap necessitates the study on the modelling of heat and moisture transfer during the concurrent open sun and two GSTESM integrated solar/sun drying processes of plantain slices in forced convection mode. The objectives of this study, therefore, are to determine drying kinetics, effective moisture diffusivity, activation energy, heat and mass transfer parameters and other related properties during the solar drying process of plantain slices.

2.0 MATERIALS AND METHODS

2.1 Sample Preparation and Drying Procedure

Samples of the fresh plantain were from the Teaching and Research Farm of Landmark University in Omu Aran, Nigeria. The Teaching and Research Farm at Landmark University in Omu Aran, which is situated at latitude 8º 8' N, and longitude 5º 5' E is where the tests were conducted. As illustrated in Figure 1, the plantains were manually peeled and then cut using a mechanical slicer to a thickness of 3 mm ± 0.5 mm[3] and spread in the tray of each dryer after being thoroughly cleaned. Following AOAC standards, the slices were oven-dried at 105 ºC to determine their initial moisture levels using the A&D company's N92 moisture analyzer[24]. The controlled dryer (A) with the plywood drying chamber allowed for solely convective heating from the solar air heater. The controlled dryer (B) with the Perspex glass drying chamber allowed for both convection heating from the solar air heater (collector) and direct radiation to dry the clean cassava slices. However, the drying in the open sun (C) involved the exposure of the plantain slices to direct radiation. For the three cases (open sun and the two controlled dryers), a clean stainless tray was covered with a layer of around 3 mm thick plantain slices of the original mass that had already been established. The drying period ran from 9:00 until 18:00. At 18:00 hrs, the plantain slices in the open sun were covered and also, the air intake vents of the controlled dryers were closed to prevent moisture reabsorption. Thereafter, the plantain slices were left to moderate at room temperature until 9:00 hrs the following day when the drying process was scheduled to commence.

A multi-channel temperature meter (AX 4202) was used to measure the temperatures of the collector, drying chamber, product, and chimney output inside the dryers at one-hour intervals. Data on solar radiation, air velocity, ambient temperature, and relative humidity were recorded hourly during the experimental periods using instruments like a pyranometer, an anemometer, and temperature and humidity sensors by the Campbell weather station (with Data logger model No: 18728). The data was then gathered from a computer system that was directly connected to the logger. Using an electronic weight balance (Model No.: D0630/30; Control S.R.L. Aosta 6 Cernusco, Italy: 30 kg, S/N 13237130091), the weight of the slice was recorded every two hours until a constant weight was reached. Based on weight loss on a wet basis, the moisture content was calculated using Eqn. (5) [24]. Table 1 gives the specifications and sensitivities of measuring devices. To achieve an average value for analysis, each measurement was made three times.

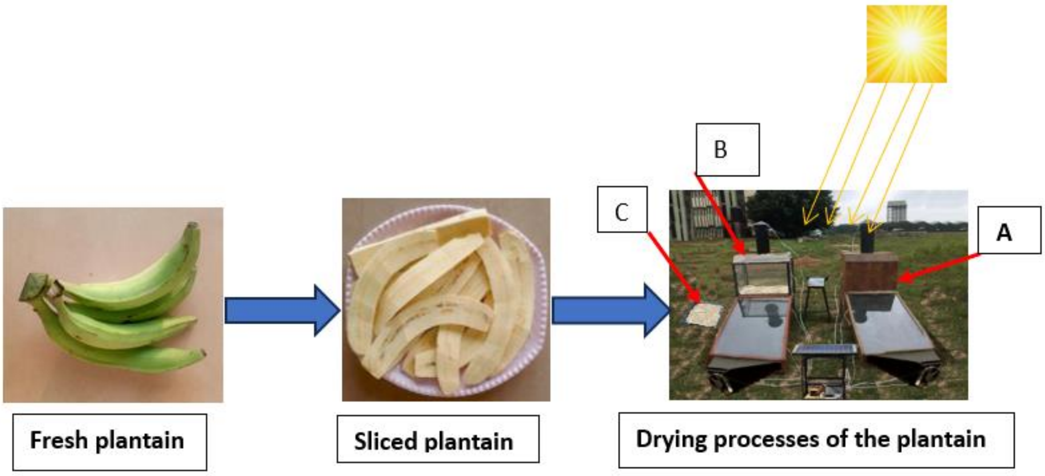

Fig.1. Graphical description of the sample preparation and drying procedure

2.2 Controlled dryer Experimental Setup Description

Two 4 kilogram tray capacity controlled dryers (A and B) with the same design but different drying chamber materials (Plywood and Perspex) make up the experimental setup, as seen conceptually and visually in Figure 2. Both comprise the base frame, a drying chamber (760 x 540 x 15) mm fabricated of plywood and Perspex, and a solar collector measuring 1470 x 840 x 80 mm. The lower section of the drying chambers (under the drying tray) was filled with granite sensible thermal energy storage material (GSTESM) to absorb heat when the solar irradiance is high and release it when the insolation is low to keep the drying chamber temperature above the ambient. All of the connections between these components were tightly sealed to minimize infiltration losses.

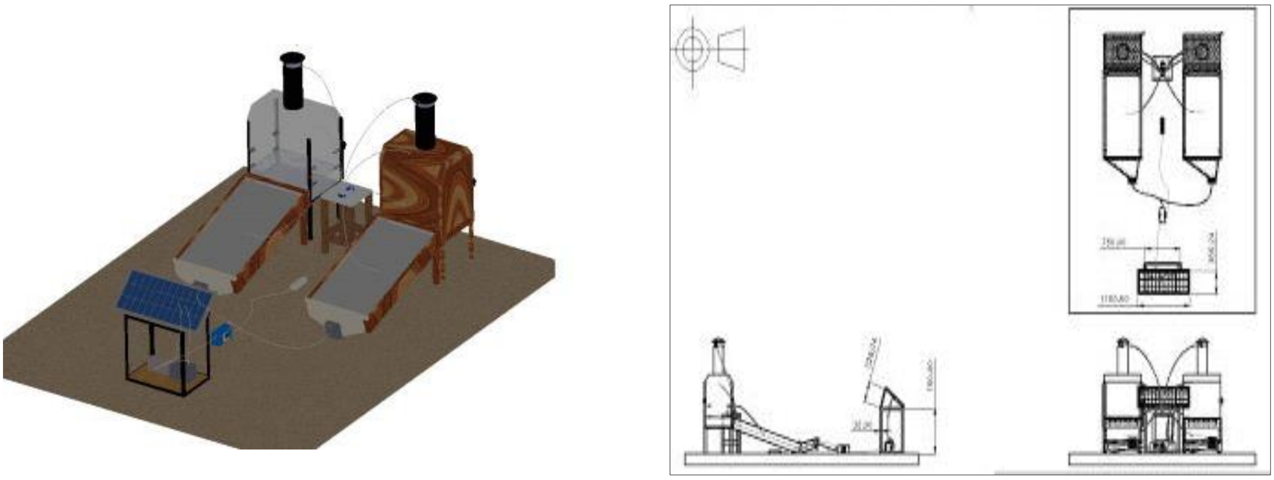

Fig.2: Isometric and Orthographic views of the controlled dryer experimental setup

Table 1: Specifications and sensitivities of measuring devices[3]

Measuring Devices	Measured parameters	Model	Sensitivity	
	Solar radiation	Data logger model	± 1 w/m^2	Campbell Scientific, UK
	Air velocity	No: 18728	± 0.1 m/s	
Campbell Weather Station	Humidity		± 1%	
Digital weighing Balance	Mass	Model No: D0630/30	± 0.01 g	Cernusco, Italy
Digital Multi-channel temperature meter	Temperature	K-type Model: AT 4208	± 0.5 ºC	Changzhou, China
Moisture analyser	Moisture content	Model: MX- 50	± 0.1 ºC	A&D Company Ltd. Japan
Lab. Air- Air-ventilated oven	Moisture content	UF. 75 Memmert	± 0.1 ºC	Schwabach, Germany

2.3 Drying kinetics

The moisture content on a wet basis (M) as a result of weight loss was determined using equation (1) [24, 25]

$$M = \frac{W_{int} - W_{bd}}{W_{int}} \quad (1)$$

where M is the moisture content (% w.b); W_{int} the initial weight of the sample (g) and W_{bd} represents the bone dried weight of the sample (g).

Using Equation (2), the dimensionless moisture ratio (MR) of cassava slices was obtained following[26] as:

$$MR = \frac{M_{ti} - M_{equ}}{M_{int} - M_{equ}} \quad (2)$$

where M_{ti}, M_{int} and M_{equ} are moisture contents measured at time t, initial moisture content, and equilibrium moisture content respectively. The value of M_{equ} is very small compared to M_{ti} or M_{int} for a long drying time. Thus Eqn. (2) can be written in a more simplified form as:

$$MR = \frac{M_{ti}}{M_{int}} \quad (3)$$

Applying Fick's second law of diffusion, plantain slices' drying rate (DR) was computed [14] and can be attributed to the unsteady-state unidimensional diffusion approach which defines the amount of moisture removed from the sample per unit time.

$$DR = \frac{M_{ti} - M_{ti+dt}}{dt} \quad (4)$$

where M_{ti+dt} is moisture content (g water/g wet solid) at $t_i + dt$, t is the time (hr) and dt is the time difference (hr).

2.4 Effective moisture diffusivity

In terms of fluid diffusion, vapour diffusion, hydrodynamic movement, and other possible mass transfer mechanisms, effective moisture diffusivity is an all-encompassing feature of moist mass transportation [27]. To match experimental data and calculate the effective moisture diffusivity, the solution of Fick's second law of diffusion in Equation (5) was used [28-30]:

$$MR = \frac{M_{ti} - M_{eq}}{M_{in} - M_{eq}} = \frac{8}{\pi^2} \sum_{n=0}^{\infty} \frac{1}{(2n+1)^2} exp\left(-\frac{(2n+1)^2 \pi^2 D_{ef} t}{4L^2}\right) \quad (5)$$

For the logarithm version of eqn. (5), the analytical solution over extended drying durations is as follows:

$$\text{Ln(MR)} = \frac{8}{\pi^2} - \frac{\pi^2 D_{ef} t}{4L^2} \quad (6)$$

where the moisture ratio is represented by MR, the effective moisture diffusivity by D_{ef}, and the half thickness of the plantain slices by L.

The obtained slope from a plot of ln (MR) against the drying time gives the effective moisture diffusivity, and it is expressed as:

$$\text{k} = \frac{\pi^2 D_{ef} t}{4L^2} \quad (7)$$

where k is the slope of the ln (MR) against time.

2.5 Activation energy

In a drying process, the activation energy is the equivalent of a potential barrier that needs to be overcome for the reaction to proceed[3]. An Arrhenius relation of the type shown in equation (8) governs how effective moisture diffusivity is dependent upon drying temperature. The pre-exponential factor and the activation energy were obtained by solving equation (8) using the Microsoft Solver tool on Excel [14]

$$D_{ef} = D_f Exp\left(-\frac{E_{ac}}{RT}\right) \quad (8)$$

where T is the absolute temperature of the air, R stands for the universal gas constant, D_f is the pre-exponential factor of the Arrhenius equation, D_{ef} is the effective moisture diffusivity, and Eac is the activation energy.

2.6 Determination of heat and mass transfer parameters

A basic method was used to simplify the numerous transient diffusion equations for heat and moisture diffusion, which were empirically calculated based on certain assumptions for different geometric shape coordinates [31]. However, most often, the equations are simplified by adopting a more general technique[32] as detailed below.

2.6.1 Heat and mass transfer coefficients

The most common approach to calculate the heat transfer coefficient of most food materials is to combine the heat and mass transfer coefficient with the Lewis number [33].

The mass transfer coefficient (H_{mo}) was determined using equation (9)[34].

$$H_{mo} = \frac{v_{ol}}{T_{SA}} \ln(MR) \quad (9)$$

where v_{ol} is the volume of the drying object (m^3) and T_{SA} is the total surface area of the object.

Similarly, the heat transfer coefficient (H_{TC}) was calculated using equation (10) following[34].

$$H_{TC} = h_{mo} \frac{k}{D_{ef} Le^{\frac{1}{3}}} \quad (10)$$

$$L_e = \frac{\alpha}{D_{ef}} \quad (11)$$

where D_e (m^2/s) and Le are the effective moisture diffusivity and Lewis number respectively and α (m^2/s) is the thermal diffusivity of the air. The Lewis number represent the measure of the relative thermal concentration boundary layer thickness.

Table 2: Average thermophysical properties values for plantain [35]

Properties			
Density (kg/m^3)	Thermal conductivity (Wm^{-1} ^{o}C^{-1})	Specific heat capacity (kJ^{-1} ^{o}C^{-1})	Thermal Diffusivity (m^2/s)
200	0.0374	2.6065	7.230 x 10^{-8}

2.7 Modelling

Table 3 displays fifteen (15) verified semi-theoretical models for modeling the drying curves of cassava slices. These models are often taken from Newton's rule of cooling and Fick's second law. Using the non-linear regression analysis curve fitting solver in Excel (2022 version), the model equations were validated and fitted to the experimental data to determine statistical parameters such as (R^2), (χ^2), (RMSE), SEE, and (SSE) which stand for coefficient of determination, reduced chi-square, root mean square error, standard error of estimate, and sum of square error, respectively (Eqns. 12 - 16). The higher R^2 values and lower χ^2, RMSE, and SSE values were chosen as the criteria for goodness of fit [14, 26, 36, 37].

$$R^2 = \frac{\sum_{i=1}^{N}(MR_i - MR_{calc,i}).\sum_{i=1}^{N}(MR_i - MR_{expt,i})}{\left[\sum_{i=1}^{N}(MR_i - MR_{calc,i})^2\right].\left[\sum_{i=1}^{N}(MR_i - MR_{expt,i})^2\right]} \quad (12)$$

$$RMSE = \left(\frac{1}{N}\sum_{i=1}^{N}\left(MR_{calc,i} - MR_{expt,i}\right)^2\right)^{\frac{1}{2}} \quad (13)$$

$$\chi^2 = \frac{\sum_{i=1}^{N}\left(MR_{calc,i} - MR_{expt,i}\right)^2}{N-m} \quad (14)$$

Table 3: Selected thin layer drying curve models considered [3]

Model Name	Model equation	References
Newton	MR= exp(-ft)	[26]
Henderson and Pabis	MR= a exp(-ft)	[14, 26]
Page	MR = $\exp(-ft^n)$	[38, 39]
Logarithmic	MR = a exp(-ft) + c	[38, 39]
Two Term	MR = a $\exp(-f_0t)$ + b $\exp(-f_1t)$	[14, 39]
Verma et al.	MR = a exp(-ft) + (1-a) exp(-gt)	[40]
Diffusion Approach	MR = a exp(-ft) + (1-a) exp(-fbt)	[37, 41]
Midili et al.	MR = a $\exp(-ft^n)$ + bt	[42]
Wang and Singh	MR = 1+ at + bt^2	[43]
Hii et al.	MR = a $\exp(-f_1t^n)$ + b exp $(-f_2t^n)$	[44]
Modified Henderson and Pabis	MR= a exp(-ft) + b exp(-gt) + c exp(-ht)	[45]
Modified Page I	MR = exp $(-(ft)^n)$	[26]
Modified Page II	MR = f exp $(-a(t/l)^n)$	[44]
Two-term Exponential	MR = a exp(-ft) + (1-a) exp(-fat)	[26]
Peleg	MR = $a(a_w^b) + c(a_w^d)$	[46]

3.0 RESULTS AND DISCUSSION

3.1 Drying kinetics

Fig. 3 depicts the variation of moisture contents (w.b.) with the drying time during the open air/solar drying processes of plantain slices. As reported for most of agricultural products, it is noticed that the moisture content falls exponentially over time[47]. The moisture content of plantain slices took 1140 minutes for both open air and solar drying system with plywood drying chamber to reduce from 61.5% to 6.83 and 7.34% w.b. respectively, while it took the solar drying system with Perspex glass chamber 1080 minutes to reduce the same initial moisture content of plantain slices to 6.13%. Generally speaking, the three drying processes took place during the falling-rate period. This suggests that the primary physical process controlling the transport of moisture in the drying samples is diffusion[25].

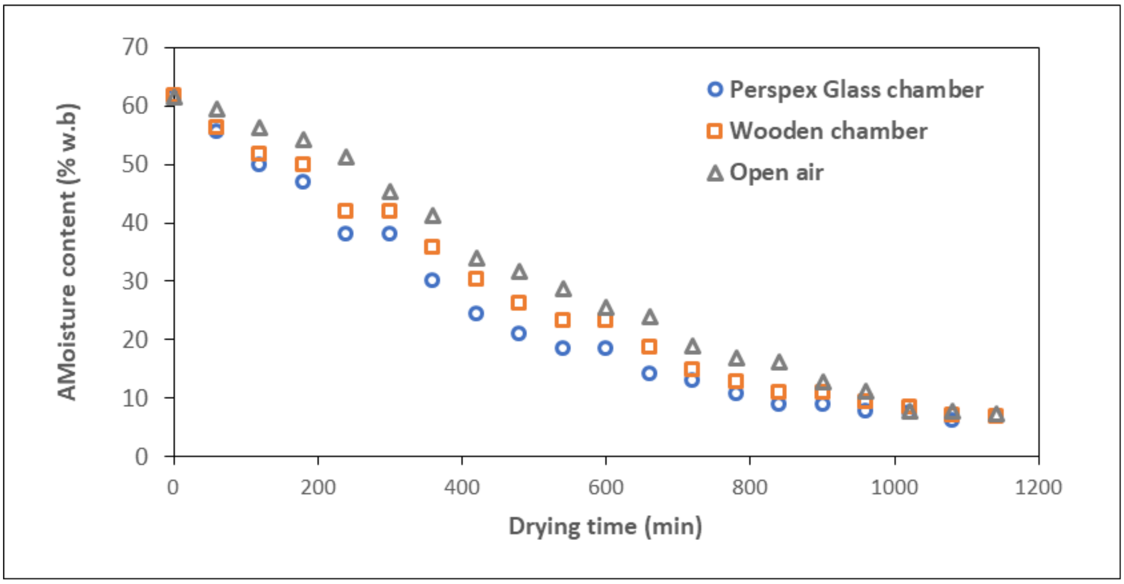

Fig. 3: Plot of moisture content against drying time

Fig. 4 presents the variation of moisture ratio with drying time. It was observed that ss drying time increased, the moisture ratio decreased, which suggests that internal mass transfer was controlled by diffusion. The continuous decrease in the moisture ratio showed that the sun/solar drying of plantain exhibit a falling curve behaviour. This is consistent with studies on the drying of agricultural goods, such as plantain chips [48] and chilli pepper[36].

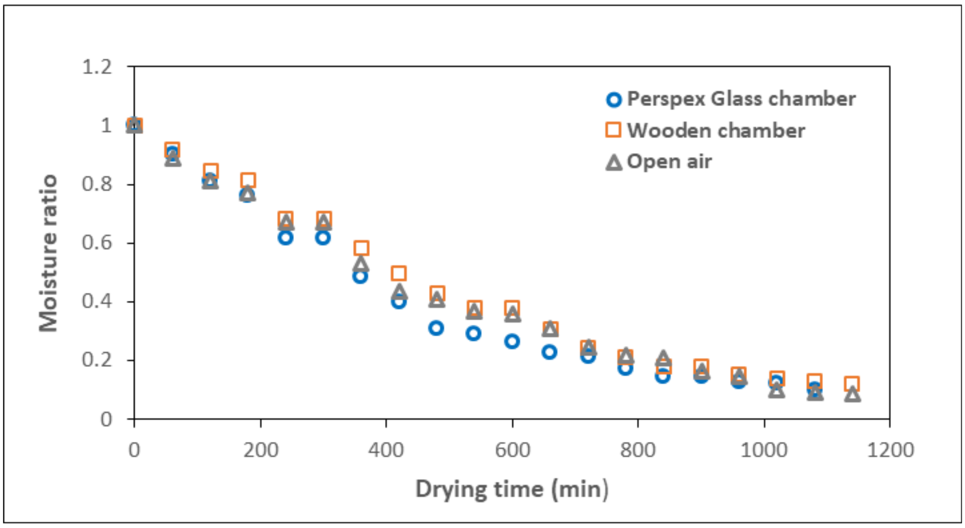

Fig. 4: Variation of moisture ratio with drying time

Fig. 5 explains the drying rate against the drying time. As anticipated, the drying temperature had a major influence on the kinetics of plantain slices drying. The drying rate exhibited sinusoidal behaaviour, which indicate the non isothermal characteristic of sun/solar dryers. This is attributed to the unpredicted weather condition. The maximum drying rate was obtained at the first 240 minutes but decreased as the drying process progresses. Generally, the rate of drying decreased as the water content reduced during the drying process. This observation is similar to he report on locust beans[12], cassava slices[3].

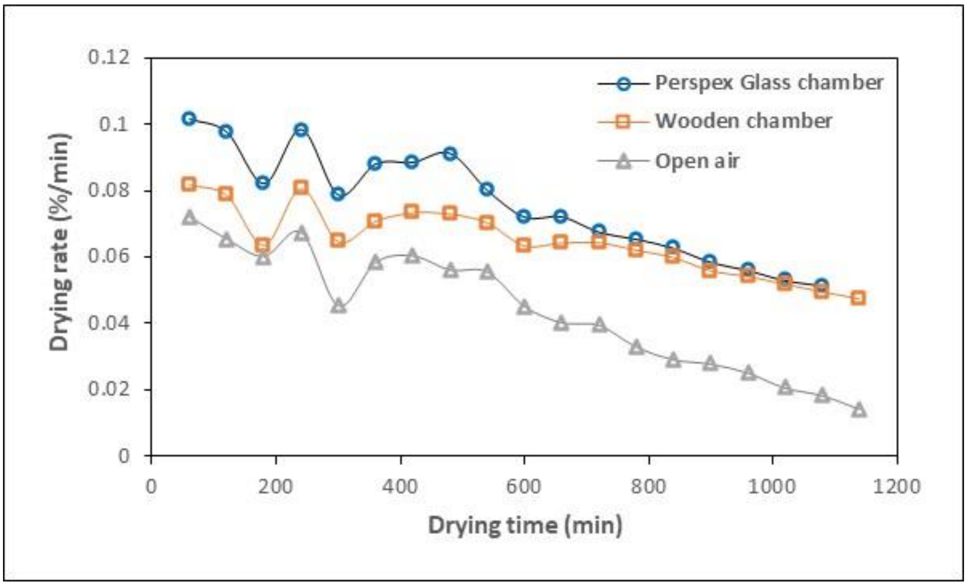

Fig. 5: Plot of drying rate versus drying time

3.2 Effective moisture diffusivity

The effective moisture diffusivities for plantain slices as indicated in Table 2 were 17.825 x 10^{-10} , 14.880 x 10^{-10} and 13.662 x 10^{-10} for the controlled solar dyers (with Perspex glass chamber, plywood chamber) and open air respectively. The greatest effective moisture diffusivity value that was obtained during the solar drying process with Perspex glass chamber. That is, an increase in drying air temperature led to an increase in effective diffusivity[14, 25]. The values of D_e obtained from this study fall within the general range 10^{-12} to 10^{-8} m^2/s for the drying of cocoa beans, garlic slices and food materials [49-51]. Also, for cassava starch, figs, and organic apple slices, the effective diffusivity value lies within the range 3×10^{-10}, 2.47×10^{-10}, and 2.2×10^{-10}, [52-54] respectively.

3.3 Activation energy

Also, Table 5 depicts the obtained activation energy with open air and solar drying systems containing Perspex and plywood chambers. The obtained activation energy values for the three drying processes (solar drying with Perspex and plywood chambers) and open air were 22.641, 22.144 and 21.983 kJ/mol. These values are close to those reported for cocoa beans, cassava slices and cassava starch [3, 14, 53].

Table 4: Effective moisture diffusivities, pre-exponential factors, activation energies for the dried plantain slices in the open air and solar dryer with different chamber materials

Parameter	Perspex glass	Wooden chamber	Open air
D_{eff} (x $10^{-10}m^2/s$)	17.825	14.880	13.622
D_o (x $10^{-10}m^2/s$)	17.665	14.753	13.504
Ea (kJ/mol)	22.641	22.144	21.983

3.3 Heat and Mass Transfer Coefficients

The values of mass transfer coefficient for the dried plantain slices in the solar drying systems (with Perspex and plywood chambers) and open air were 1.246 x 10^{-6}, 1.435 x 10^{-6}, 1.966 x 10^{-6} m/s respectively. While the heat transfer coefficients were 3.165, 3.0412 and 2.751 W/m^2. K. The obtained values fall within the available range in the literature for cassava slices [3]. The solar drying system with Perspex chamber had the highest rate of heat and moisture transfer than plywood chamber solar dryer and the open air.

3.4 Modelling

Tables 5 gives the results of the non-linear regression analysis from the chosen thin layer models utilizing open air drying and solar drying systems integrated with granite sensible thermal energy storage material (GSTESM). The Table displays fifteen (15) chosen drying models along with their derived constants, coefficients, and other statistical parameters (i.e. coefficient of determination, R^2; chi-square, χ^2 and root mean square, RMSE for the three experimental conditions. In all the tested models, the R^2 value for the solar drying experiment with Perspex drying chamber ranged from 0.814 to 0.992 (the greatest being the Midilli et al. model and the lowest being the Modified Henderson Pabis model). Similarly, the R^2 values were 0.868 and 0.995 (between the Midilli (highest) and Modified Henderson pabis (lowest) models). Aside the Modified Henderson Pabis, the R^2 values for the tested models in the three cases exceeded the acceptable threshold of 0.90 [50]. The higher values of R^2 for

Midilli et al. in the two solar drying with Perspex glass and plywood chamber and logarithmic in the open air indicate a stronger relationship between the moisture ratio and drying time than other tested models. Also, the value of χ^2 ranged between 0.0008 and 0.2341; 0.0005 and 0.2763 and 0.0014 and 0.2912 respectively for the solar drying system with chamber Perspex and plywood chamber and open air. Also, the RMSE values ranged from 0.025 to 0.814; 0.019 - 0.440 and 0.0341 and 0.872 respectively for the three processes. The results show that the Midilli et al. model gave the highest value of R^2 and the lowest values of other parameters for solar drying system with the Perspex glass and plywood chambers. while the logarithmic model gave the highest value of R^2 and the lowest values of other parameters for open air drying. It can be concluded, therefore, that the model proposed by Midilli et al. performed better than the others in describing the drying behavior of the solar drying system of plantain slices using the Perspex glass and plywood chamber, while the model proposed by logarithmic performed better than the others in describing the open air behaviour of plantain slices. The solar drying of plantain slices using Perspex glass and plywood chambers is in good agreement with the Midilli et al. model on cassava slices[3], while drying in the open air is in good agreement with logarithmic model on pistachio[55]. Therefore, these models may be assumed to represent the thin layer solar drying behaviour of plantain slices with Perspex glass and plywood chambers and open air within the experimental range of the study.

Table 5: Model constant and goodness of fit parameter of drying of plantain slices in the open air and solar dryer with different chamber materials

Dryer Chamber	Model name	Model constant	R^2	RMSE	χ^2
Perspex Glass	Newton	f = 0.1257	0.988	0.035	0.0013
	Henderson and pabis	f = 0.1313, a = 1.0411	0.988	0.032	0.0011
	Page	f = 0.0944, n = 1.1342	0.990	0.028	0.0009
	Logarithmic	f = 0.1219, a = 1.0655, c = -0.0331	0.988	0.031	0.0011
	Two term	f = 10.97 $\times10^{-5}$, g = 0.0007, a = -88.6065, c = 89.4582	0.906	0.087	0.0096
	Verma et al.	f = 0.109, g = 0.1184, a = -0.7222	0.988	0.034	0.0014
	Diffusion approach	f = 0.001, g = 32.8571, a = -1.4259	0.943	0.084	0.0084
	Midili et al.	**f = 0.0761, b = 0.0039, a = 0.988, n = 1.2893**	**0.992**	**0.025**	**0.0008**
	Wang and smith	a = -0.1033, b = 0.003	0.991	0.027	0.0008
	Hii et al.	f = 0.0973, g = 0.0223, a = 1.0059, c = 7.85 $\times10^{-5}$, n = 1.1231	0.990	0.028	0.0011
	Modified Henderson Pabis	f = 8.0899, a = 0.084, g = -5.2194, b = 0.0845, h = -1.8862, c = 0.1354	0.814	0.400	0.2341
	Modified Page I	f = 0.1248, n = 1.1332	0.990	0.028	0.0009
	Modified Page II	f = 1.0089, a = 0.0008, n = 1.1123, L = 0.013	0.990	0.028	0.0010
	Two term exponential	f = 6.3158, a = 0.0203	0.987	0.033	0.0012
	Peleg	a = 7.8312, b = 0.6351	0.984	0.037	0.0015
Wooden chamber	Newton	f = 0.1045	0.988	0.040	0.0017
	Henderson and pabis	f = 0.1115, a = 1.0578	0.987	0.033	0.0012
	Page	f = 0.0637, n = 1.2203	0.995	0.021	0.0005
	Logarithmic	f = 0.0842, a = 1.1825, c = -0.1526	0.991	0.027	0.0008
	Two term	f = 12.01 $\times10^{-5}$, g = 0.0007, a = -88.6697, c = 89.5694	0.945	0.067	0.0055
	Verma et al.	f = 0.0445, g = 0.049, a = -8.9495	0.991	0.028	0.0009

	Diffusion approach	f = 0.63 ×10⁻⁵, g = 15.5667, a = -601.4269	0.944	0.085	0.0086
	Midili et al.	**f = 0.0496, b = 0.0025, a = 0.9805, n = 1.3584**	**0.995**	**0.019**	**0.0005**
	Wang and smith	a = -0.0844, b = 0.002	0.994	0.022	0.0006
	Hii et al.	f = 0.0591, g = 0.0223, a = 0.9919, c = 7.87 ×10⁻⁵, n = 1.2489	0.995	0.021	0.0006
	Modified henderson pabis	f = 5.8097, a = -0.0231, g = 0.0356, b = -0.1031, h = -4.8396, c = -0.0305	0.868	0.440	0.2763
	Modified Page I	f = 0.1046, n = 1.2319	0.995	0.021	0.0005
	Modified Page II	f = 0.9945, a = 0.0005, n = 1.2409, L = 0.0207	0.995	0.021	0.0005
	Two term exponential	f = 4.6061, a = 0.0233	0.986	0.037	0.0015
	Peleg	a = 10.5943, b = 0.5194	0.989	0.031	0.0011
Open sun air	Newton	f = 0.109	0.9799	0.0433	0.0020
	Henderson and pabis	f = 0.1128, a = 1.0317	0.9785	0.0417	0.0019
	Page	f = 0.0748, n = 1.1662	0.9834	0.0364	0.0015
	Logarithmic	**f = 0.0777, a = 1.1996, c = -0.204**	**0.9854**	**0.0341**	**0.0014**
	Two term	f = 12.06 ×10⁻⁵, g = 0.0007, a = -88.4163, c = 89.2952	0.9480	0.0638	0.0051
	Verma et al.	f = 0.0479, g = 0.0524, a = -8.9095	0.9852	0.0342	0.0016
	Diffusion approach	f = 0.64 ×10⁻⁵, g = 15.5912, a = -602.3411	0.9474	0.0905	0.0096
	Midili et al.	f = 0.0834, b = -0.0049, a = 0.9919, n = 1.0428	0.9852	0.0341	0.0015
	Wang and smith	a = -0.0857, b = 0.002	0.9847	0.0350	0.0014
	Hii et al.	f = 0.0657, g = 0.0223, a = 0.9739, c = 7.86 ×10⁻⁵, n = 1.2101	0.9838	0.0357	0.0017
	Modified henderson pabis	f = 5.8097, a = -0.0231, g = 0.0356, b = -0.1031, h = -4.8396, c = -0.0305	0.8782	0.4515	0.2912
	Modified Page I	f = 0.1084, n = 1.1566	0.9833	0.0364	0.0015
	Modified Page II	f = 0.9682, a = 0.0005, n = 1.2318, L = 0.0195	0.9837	0.0358	0.0016
	Two term exponential	f = 5.1189, a = 0.0218	0.9776	0.0427	0.0020
	Peleg	a = 9.9782, b = 0.5428	0.9848	0.0345	0.0013

Figs. 6 and 7 depict the plot of predicted moisture ratio values against the observed moisture ratio. It can be seen that the predicted moisture ratio data from the midilli model versus the observed data for the thin layer forced convective solar drying process generally banded around the line of best fit. This further confirms that the Midilli model could be used to explain the solar drying behaviour of plantain slices within the

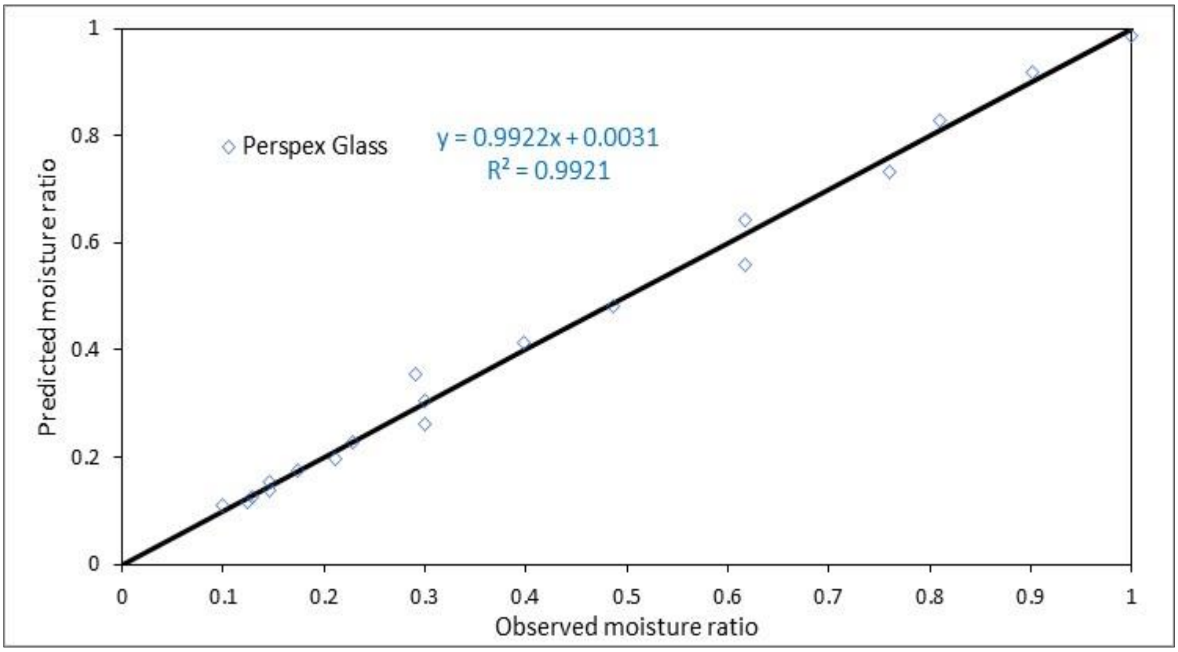

Fig. 6: Plot of the predicted MR versus observed MR for Perspex glass chamber dryer

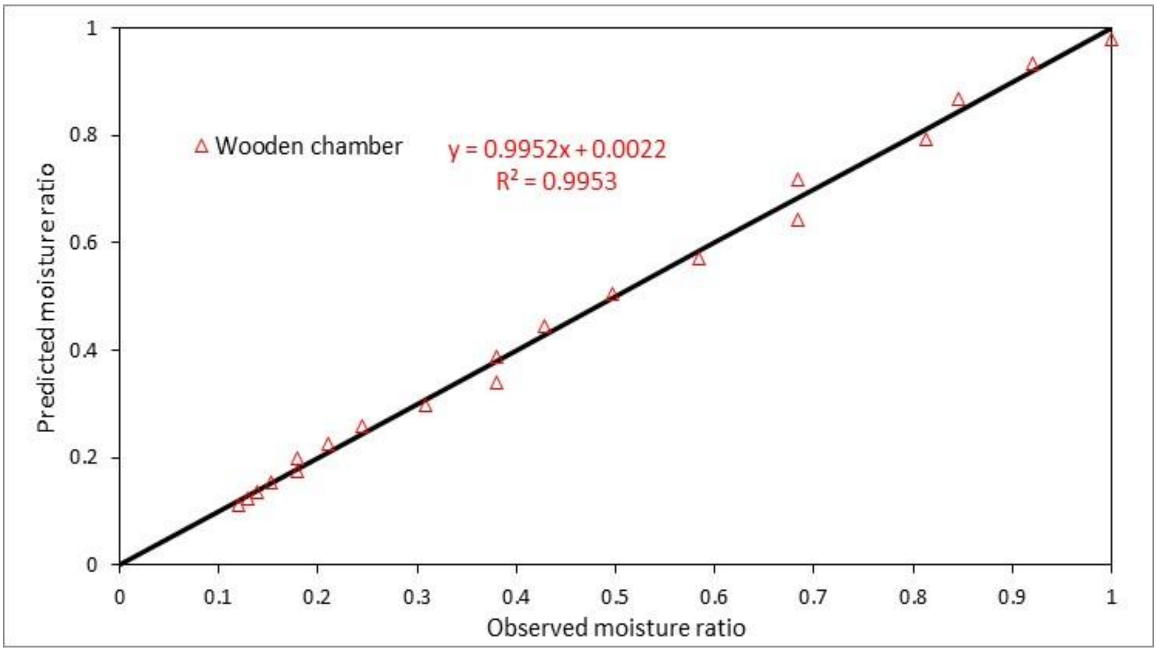

Fig. 7: Plot of the predicted MR versus experimental MR for the wooden chamber dryer

Fig. 8 depicts the plot of predicted moisture ratio values against the observed moisture ratio. It can be seen that the predicted moisture ratio data from the logarithmic model versus the observed data for the thin layer open air drying process generally banded around the line of best fit. This further confirms that the logarithmic model could be used to explain the solar drying behaviour of plantain slices within the study range.

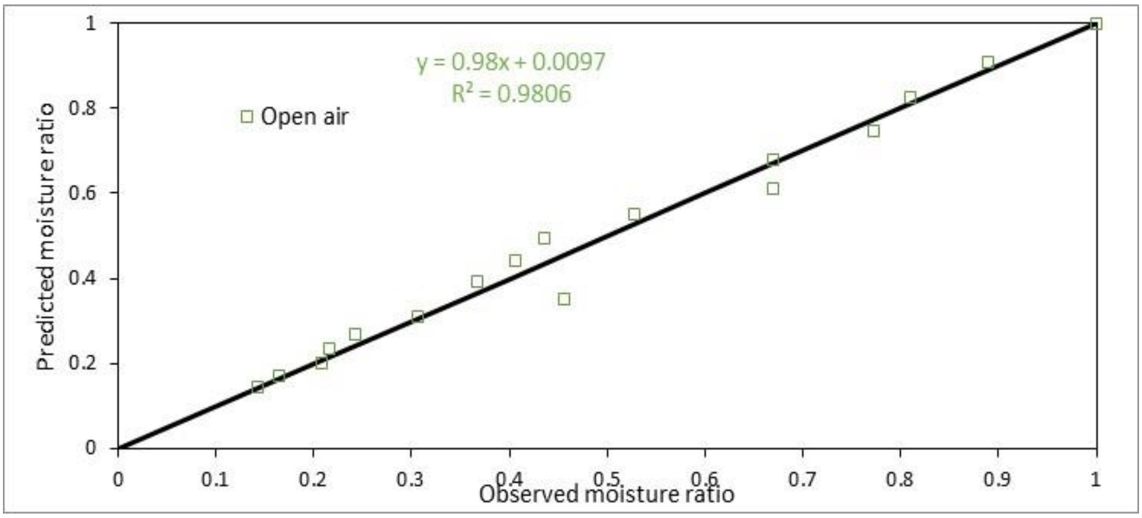

Fig. 8: Plot of the predicted MR versus experimental MR for the open

4.0 CONCLUSION

Investigations on thermo-kinetics modeling of the sun drying of plantain slices using granite thermal energy storage material under open air and forced convection conditions were conducted. For the forced convection condition, two identical solar drying systems with Perspex glass and plywood drying chambers were used in the experiment. From the experiments, the following conclusion could be drawn:

(i) The moisture content of plantain slices took 1140 minutes for both open air and solar drying system with plywood drying chamber to reduce from 61.5% to 6.83 and 7.34% w.b. respectively, while it took the solar drying system with Perspex glass chamber 1080 minutes to reduce the same initial moisture content of plantain slices to 6.13%.

(ii) The maximum drying rate was obtained at the first 240 minutes but decreased as the drying process progresses.

(iii) The effective moisture diffusivities for plantain slices were 17.825 x 10^{-10} , 14.880 x 10^{-10} and 13.662 x 10^{-10} for the controlled solar dyers (with Perspex glass chamber, plywood chamber) and open air respectively.

(iv) The obtained activation energy values for the three drying processes (solar drying with Perspex and plywood chambers) and open air were 22.641, 22.144 and 21.983 kJ/mol.

(v) The values of mass transfer coefficient for the dried plantain slices in the solar drying systems (with Perspex and plywood chambers) and open air were 1.246 x 10^{-6}, 1.435 x 10^{-6}, 1.966 x 10^{-6} m/s respectively. While the heat transfer coefficients were 3.165, 3.0412 and 2.751 W/m^2. K.

(vi) Midilli et al. performed better than the others in describing the drying behavior of the solar drying system of plantain slices using the Perspex glass and plywood chamber, while the model proposed by logarithmic performed better than the others in describing the open air behaviour of plantain slices.

(vii) The obtained results would be useful in the design of devices involving open air and sun drying of plantain slices.

REFERENCES

1. Oke, O., J. Redhead, and M. Husain, Roots, tubers, plantains and bananas in human nutritionFood and Agriculture Organization of the United Nations (FAO) and the Information Network on Post-Harvest Operations (INPhO). FAO code: 86, AGRIS: SO1, ISBN 92-5-102862-1. Science Quarterly 198pp. Rome, Italy, 1998. 198.
2. Sahay, K. and K. Singh, Unit operations of agricultural processing. 1996.
3. Komolafe, C.A., et al., Kinetics and modeling of the heat and mass transfer during the solar drying of Cassava Slices under Natural Convection mode. Journal of Thermal Science and Engineering Applications, 2025. 17(1).
4. Dinani, S.T., et al., Mathematical modeling of hot air/electrohydrodynamic (EHD) drying kinetics of mushroom slices. Energy conversion and Management, 2014. 86: p. 70-80.
5. Guiné, R.P. and R.M. Fernandes, Analysis of the drying kinetics of chestnuts. Journal of Food Engineering, 2006. 76(3): p. 460-467.
6. Komolafe, C.A., et al., Numerical Analysis of Three-Dimensional Heat and Mass Transfer in Cocoa Beans Under a Solar Drying Condition With a Thermal Storage Material. Journal of Thermal Science and Engineering Applications, 2022. 14(7).
7. Pangavhane, D.R., R. Sawhney, and P. Sarsavadia, Design, development and performance testing of a new natural convection solar dryer. Energy, 2002. 27(6): p. 579-590.
8. Simate, I., Optimization of mixed-mode and indirect-mode natural convection solar dryers. Renewable energy, 2003. 28(3): p. 435-453.

9. Hallak, H., et al., The staircase solar dryer: design and characteristics. Renewable Energy, 1996. 7(2): p. 177-183.
10. Montero, I., et al., Design, construction and performance testing of a solar dryer for agroindustrial by-products. Energy Conversion and Management, 2010. 51(7): p. 1510-1521.
11. Seveda, M., Design and development of walk-in type hemicylindrical solar tunnel dryer for industrial use. International Scholarly Research Notices, 2012. 2012.
12. Komolafe, C.A., et al., Modelling of moisture diffusivity during solar drying of locust beans with thermal storage material under forced and natural convection mode. Case Studies in Thermal Engineering, 2019. 15: p. 100542.
13. Dairo, O.U., et al., Solar drying kinetics of Cass Ava Slices in a mixed flow dryer. Acta Technologica Agriculturae, 2015. 18(4): p. 102-107.
14. Komolafe, C.A., et al., Sun drying of cocoa with firebrick thermal storage materials. International Journal of Energy Research, 2020. 44(8): p. 7015-7025.
15. Duffy, A., M. Rogers, and L. Ayompe, Renewable energy and energy efficiency: assessment of projects and policies. 2015: John Wiley & Sons.
16. Komolafe, C.A., Numerical simulation of the 3D simultaneous heat and mass transfer in a forced convection solar drying system integrated with thermal storage material. Journal of Solar Energy Engineering, 2023. 145(5).
17. Owolarafe, O.K., et al., Performance evaluation of a small-scale dryer for agricultural products. Agricultural Engineering International: CIGR Journal, 2021. 23(3).
18. Muritala, A., S. Obayopo, and S. Odediran, A study of a forced convective biomass dryer for plantain chips. Agricultural Engineering International: CIGR Journal, 2022. 24(4).
19. Ekeke, I., et al., Statistical modelling of drying characteristics of unripe plantain (Musa Paradisiaca) slices. International Journal of Engineering and Management Research (IJEMR), 2019. 9(4): p. 30-39.
20. Arinola, S., E. Ogunbusola, and S. Adebayo, Effect of drying methods on the chemical, pasting and functional properties of unripe plantain (Musa paradisiaca) flour. British Journal of Applied Science & Technology, 2016. 14(3): p. 1-7.
21. Satimehin, A., J. Alakali, and O. Alabi, Thin-layer drying characteristics of plantain (Musa paradisiaca) chips. 2010.
22. Kusuma, H.S., et al., Evaluation of drying kinetics, electric and emission study of Musa paradisiaca L. leaves using microwave-assisted drying method. Applied Food Research, 2023. 3(2): p. 100322.
23. Madukasi, A.H., et al., Optimization of the Drying Parameters for Plantain Chips using a Locally Made Tray Dryer: A Study on Drying Efficiency and Drying Rate Modeling using RSM. Journal of Food Technology & Nutrition Sciences. SRC/JFTNS-268. DOI: doi. org/10.47363/JFTNS/2025 (7), 2025. 206: p. 2-10.
24. Horwitz, W. and G. Latimer, Association of official analytical chemists.(2010). Official methods of analysis of the Association of Official Analytical Chemist. Gaithersburg, MD, USA, 2000.
25. Komolafe, C. and M. Waheed, Temperatures dependent drying kinetics of cocoa beans varieties in air-ventilated oven. Frontiers in Heat and Mass Transfer (FHMT), 2018. 12.
26. Taghian Dinani, S., et al., Drying of mushroom slices using hot air combined with an electrohydrodynamic (EHD) drying system. Drying Technology, 2014. 32(5): p. 597-605.
27. Dina, S.F., et al., Study on effectiveness of continuous solar dryer integrated with desiccant thermal storage for drying cocoa beans. Case Studies in Thermal Engineering, 2015. 5: p. 32-40.
28. Kituu, G.M., et al., Thin layer drying model for simulating the drying of Tilapia fish (Oreochromis niloticus) in a solar tunnel dryer. Journal of Food Engineering, 2010. 98(3): p. 325-331.
29. Bahammou, Y., et al., Thin-layer solar drying characteristics of Moroccan horehound leaves (Marrubium vulgare L.) under natural and forced convection solar drying. Solar Energy, 2019. 188: p. 958-969.
30. Dissa, A., et al., Modelling and experimental validation of thin layer indirect solar drying of mango slices. Renewable energy, 2009. 34(4): p. 1000-1008.
31. Ndukwu, M.C., et al., Heat and mass transfer parameters in the drying of cocoyam slice. Case Studies in Thermal Engineering, 2017. 9: p. 62-71.
32. Miller, W.M., Prediction of energy requirements and drying times for surface drying fresh produce. 1985.
33. Camargo, J., C. Ebinuma, and S. Cardoso, A mathematical model for direct evaporative cooling air conditioning system. Engenharia Termica, 2003. 4: p. 30-34.
34. Gilago, M.C., V.R. Mugi, and V. Chandramohan, Evaluation of drying kinetics of carrot and thermal characteristics of natural and forced convection indirect solar dryer. Results in Engineering, 2023. 18: p. 101196.

35. Essien, E., et al., Investigation of thermal properties of plantain (Musa paradisiaca) and Mfang Aya (Thaumatococcus daniellii) as thermal radiation insulator. J. Nat. Sci. Res, 2016. 6(15): p. 33-37.
36. Tunde-Akintunde, T., Mathematical modeling of sun and solar drying of chilli pepper. Renewable energy, 2011. 36(8): p. 2139-2145.
37. Doymaz, İ., Convective air drying characteristics of thin layer carrots. Journal of food engineering, 2004. 61(3): p. 359-364.
38. Asemu, A.M., et al., Drying characteristics of maize grain in solar bubble dryer. Journal of Food Process Engineering, 2020. 43(2): p. e13312.
39. Akgun, N.A. and I. Doymaz, Modelling of olive cake thin-layer drying process. Journal of food Engineering, 2005. 68(4): p. 455-461.
40. Verma, L.R., et al., Effects of drying air parameters on rice drying models. Transactions of the ASAE, 1985. 28(1): p. 296-0301.
41. Doymaz, I., An experimental study on drying of green apples. Drying technology, 2009. 27(3): p. 478-485.
42. Midilli, A., H. Kucuk, and Z. Yapar, A new model for single-layer drying. Drying technology, 2002. 20(7): p. 1503-1513.
43. Wang, C. and R. Singh, A single layer drying equation for rough rice. 1978. ASAE paper.
44. Hii, C., C. Law, and M. Cloke, Modeling using a new thin layer drying model and product quality of cocoa. Journal of food engineering, 2009. 90(2): p. 191-198.
45. Kaleta, A. and K. Górnicki, Evaluation of drying models of apple (var. McIntosh) dried in a convective dryer. International journal of food science & technology, 2010. 45(5): p. 891-898.
46. Peleg, M., A mathematical model of crunchiness/crispness loss in breakfast cereals 1. Journal of Texture Studies, 1994. 25(4): p. 403-410.
47. Toujani, M., et al., Experimental study and mathematical modeling of silverside fish convective drying. Journal of Food Processing and Preservation, 2013. 37(5): p. 930-938.
48. Mier, M.V., et al., Modeling of drying kinetics of ripe plantain (Musa paradisiaca) chips in a forced convection tunnel: Modelización de la cinética de secado de astillas de plátano maduro (Musa paradisiaca) en un túnel de convección forzada. South Florida Journal of Environmental and Animal Science, 2022. 2(4): p. 294-304.
49. Komolafe, C.A. and M.A. Waheed. Design and fabrication of a forced convection solar dryer integrated with heat storage materials. in ACSM. 2018.
50. Madamba, P.S., R.H. Driscoll, and K.A. Buckle, The thin-layer drying characteristics of garlic slices. Journal of food engineering, 1996. 29(1): p. 75-97.
51. Zogzas, N., Z. Maroulis, and D. Marinos-Kouris, Moisture diffusivity data compilation in foodstuffs. Drying technology, 1996. 14(10): p. 2225-2253.
52. Doymaz, I., Sun drying of figs: an experimental study. Journal of Food Engineering, 2005. 71(4): p. 403-407.
53. Suherman, S., et al., Energy–exergy analysis and mathematical modeling of cassava starch drying using a hybrid solar dryer. Cogent Engineering, 2020. 7(1): p. 1771819.
54. Sacilik, K. and A.K. Elicin, The thin layer drying characteristics of organic apple slices. Journal of food engineering, 2006. 73(3): p. 281-289.
55. Midilli, A. and H. Kucuk, Mathematical modeling of thin layer drying of pistachio by using solar energy. Energy conversion and Management, 2003. 44(7): p. 1111-1122.